

## The effect of Zr addition on the formation and structural properties of 3:29 compounds in the Fe–Nd–Ti–Zr system

This article has been downloaded from IOPscience. Please scroll down to see the full text article.

2005 J. Phys.: Condens. Matter 17 6007

(<http://iopscience.iop.org/0953-8984/17/38/006>)

View [the table of contents for this issue](#), or go to the [journal homepage](#) for more

Download details:

IP Address: 129.252.86.83

The article was downloaded on 28/05/2010 at 05:58

Please note that [terms and conditions apply](#).

# The effect of Zr addition on the formation and structural properties of 3:29 compounds in the Fe–Nd–Ti–Zr system

S B Han<sup>1</sup>, J Y Lv<sup>1</sup>, X F Liu<sup>1</sup>, J Peng<sup>1</sup>, X J Li<sup>1</sup>, D F Chen<sup>2</sup>, Y J Xue<sup>2</sup>,  
J H Li<sup>2</sup> and Z B Hu<sup>1</sup>

<sup>1</sup> College of Chemistry and Chemistry Engineering, Graduate School of Chinese Academy of Science, Beijing 100049, People's Republic of China

<sup>2</sup> China Institute of Atomic Energy, Beijing 102413, People's Republic of China

Received 16 June 2005, in final form 27 July 2005

Published 9 September 2005

Online at [stacks.iop.org/JPhysCM/17/6007](http://stacks.iop.org/JPhysCM/17/6007)

## Abstract

A new series of 3:29 compounds in the Fe–Nd–Ti–Zr quaternary system were synthesized successfully. The formation and structural properties were studied by means of powder x-ray and powder neutron diffraction. The results reveal that only a small amount of Zr content can exist in the 3:29-type compounds in the Fe–Nd–Ti–Zr quaternary system. Higher Zr content induces the formation of rhombohedral Th<sub>2</sub>Zn<sub>17</sub>-type phase. In the structures of 3:29-type compounds, the Zr content partially substitutes for Nd and enters the 2a and 4i crystallographic sites exclusively. Upon Zr substitution, the lattice parameters *a*, *b*, *c* and the unit cell volumes *V* of (Nd, Zr)<sub>3</sub>(Fe, Ti)<sub>29</sub> compounds decrease monotonically and their intrinsic magnetic properties, including the Curie temperature and saturation magnetization, lessen as well.

## 1. Introduction

R<sub>3</sub>(Fe, M)<sub>29</sub>-type compounds (R = Y, Ce, Pr, Nd, Sm, Gd, Tb, Dy and M = Ti, V, Cr, Mn, Nb, Mo, Ta, W, Re [1–7]) have attracted much interest recently in view of their promise for permanent magnet applications. R<sub>3</sub>Fe<sub>29</sub> is non-existent and a third transitional metal element M, namely the stabilizing element, is indispensable for stabilizing the monoclinic structure with *A2/m* space group [8–11]. The 3:29-type structure can be derived from alternate stacking of the rhombohedral Th<sub>2</sub>Zn<sub>17</sub>-type and the tetragonal ThMn<sub>12</sub>-type units. In fact, the three structure types are all derivatives of the RFe<sub>5</sub> compound (CuCa<sub>5</sub>-type structure), obtained by appropriate replacement of a fraction of R atoms by Fe–Fe dumbbells. There are two formula units and 64 atoms per unit cell of 3:29 phase with two crystallographically nonequivalent R sites and eleven crystallographically nonequivalent Fe(M) sites. The stabilizing element M has a strong preference for occupying the 4i<sub>1</sub>, 4i<sub>2</sub> and 4g sites as a result of the size effect (the volume of the site) and the thermodynamic

effect (the atomic environment). Both the rare earth R and the stabilizing element M have detrimental influences on the structural and magnetic properties. Many investigations on substitution of various rare earth or stabilizing elements, such as  $\text{Nd}_{3-x}\text{Dy}_x(\text{Fe}, \text{Ti})_{29}$  [12],  $(\text{Y}_{1-x}\text{Gd}_x)_3\text{Fe}_{27.5}\text{Ti}_{1.5}$  [13],  $(\text{Nd}_{1-x}\text{Tb}_x)_3\text{Fe}_{27.31}\text{Ti}_{1.69}$  [14],  $(\text{Sm}_{1-x}\text{Pr}_x)_3\text{Fe}_{27.5}\text{Ti}_{1.5}$  [15],  $(\text{Nd}_{1-x}\text{Ho}_x)_3\text{Fe}_{27.31}\text{Ti}_{1.69}$  [16],  $(\text{Nd}_{1-x}\text{Er}_x)_3\text{Fe}_{27.31}\text{Ti}_{1.69}$  [17],  $(\text{Nd}_{1-x}\text{Y}_x)_3\text{Fe}_{27.31}\text{Ti}_{1.69}$  [18],  $\text{Pr}_2\text{Er}(\text{Fe}, \text{Ti})_{29}$ ,  $\text{SmNd}_2(\text{Fe}, \text{Ti})_{29}$  [19],  $(\text{Gd}_{1-x}\text{R}_x)_3\text{Fe}_{27.31}\text{Ti}_{1.69}$  ( $\text{R} = \text{Ce}, \text{Nd}, \text{Sm}$ ) [20],  $\text{Nd}_3\text{Fe}_{27.5}\text{Ti}_{1.5-y}\text{Mo}_y$  [9] and  $\text{Gd}_3(\text{Fe}, \text{Ni})_{28}$  ( $\text{Nb}, \text{Mo}$ ) [21], have been reported.

As a transition element, Zr is of much interest because of its covalent radius (1.45 Å): larger than those of Fe (1.17 Å), Ti (1.32 Å) and Mo (1.29 Å), but smaller than that of Nd (1.64 Å). Zr has been tried for replacing R, Fe or M in different structures. For example, the addition of Zr in the  $\text{Nd}_2\text{Fe}_{14}\text{B}$  compounds, such as  $\text{Nd-Fe-B-Zr}$  [22] and  $\text{Nd-Dy-Fe-B-Zr}$  [23], has been reported. In the case of  $\text{Th}_2\text{Zn}_{17}$ -type compounds,  $(\text{Sm} + \text{Zr})_2\text{Co}_{17}$  [24],  $\text{Sm}_2\text{Fe}_{15}\text{Zr}_2$  [25],  $\text{Nd}_2\text{Fe}_{17-x}\text{Zr}_x$  [26] and  $\text{Nd}_{2-x}\text{Zr}_x\text{Fe}_{17}$  [27] have been synthesized. For the  $\text{ThMn}_{12}$ -type alloys,  $\text{Nd}(\text{Fe}, \text{Mo}, \text{Zr})_{12}$  [28] and 1:12-type compounds in the  $\text{Fe-Gd-Mo-Zr}$  system [29] have been investigated. Additionally, 1:7-type  $\text{Sm-Co-Zr}$  [30] has also been prepared. Structural investigations of these compounds reveal that almost all the Zr atoms occupy the R sites, while only a small fraction of them enter the  $\text{Fe}(\text{Mo})$  sublattice. Up to now, little attention has been paid to studying the effect of Zr addition on the formation and the structural and magnetic properties of 3:29-type compounds. In this study, a new series of 3:29-type compounds ( $x \leq 0.3$ ) in the  $\text{Fe-Nd-Ti-Zr}$  quaternary system were synthesized successfully. The dependences of the phase formation on Zr and the crystallographic properties were investigated by means of powder x-ray diffraction and powder neutron diffraction. The Curie temperatures and saturation magnetization at room temperature for the compounds are also presented.

## 2. Experimental procedure

Samples with stoichiometric compositions  $\text{Nd}_{3-x}\text{Zr}_x\text{Fe}_{27.5}\text{Ti}_{1.5}$  ( $0 \leq x \leq 1.0$ ) were prepared by arc melting under a high purity Ar atmosphere. The ingots were remelted at least four times to promote homogeneity. The purities of all the constituent elements is 99% or higher. An excess amount (about 5 wt%) of rare earth was added in order to compensate for the weight loss during arc melting. The as-cast ingots were sealed into a ceramic tube filled with high purity Ar and annealed for 24 h at from 1273 to 1323 K and then quenched in water.

X-ray and neutron powder diffraction studies were carried out to determine the crystallographic structure and phase components. X-ray powder diffraction data were collected on MSAL-XD2 with  $\text{Cu K}\alpha$  radiation at the Laboratory of Inorganic Materials of the Graduate School of the Chinese Academy of Sciences. Neutron powder diffraction data were collected on the Special Environment Powder Diffractometer (SEPD) at room temperature at Argonne's Intense Pulsed Neutron Source (IPNS). The XRD patterns are refined using the program FULLPROF [31] and the neutron diffraction patterns are refined with the program GSAS [32]. In view of the negligibly small contribution of the magnetic moments, they were neglected during the refinement of the neutron diffraction patterns. Magnetic measurements were done in a vibrating sample magnetometer (VSM) at the Institute of Physics, Chinese Academy of Sciences. The thermomagnetic analyses (TMA) were performed in a low field of 0.1 T at temperatures ranging from room temperature to above the Curie temperature and the saturation magnetization was measured at room temperature in magnetic fields up to 2 T.

## 3. Results and discussion

Figure 1 shows the XRD patterns of samples with different Zr contents ( $0.1 \leq x \leq 0.4$ ). It can be seen that at  $x \leq 0.3$  the main phases crystallize in a monoclinic  $\text{Nd}_3(\text{Fe}, \text{Ti})_{29}$ -type

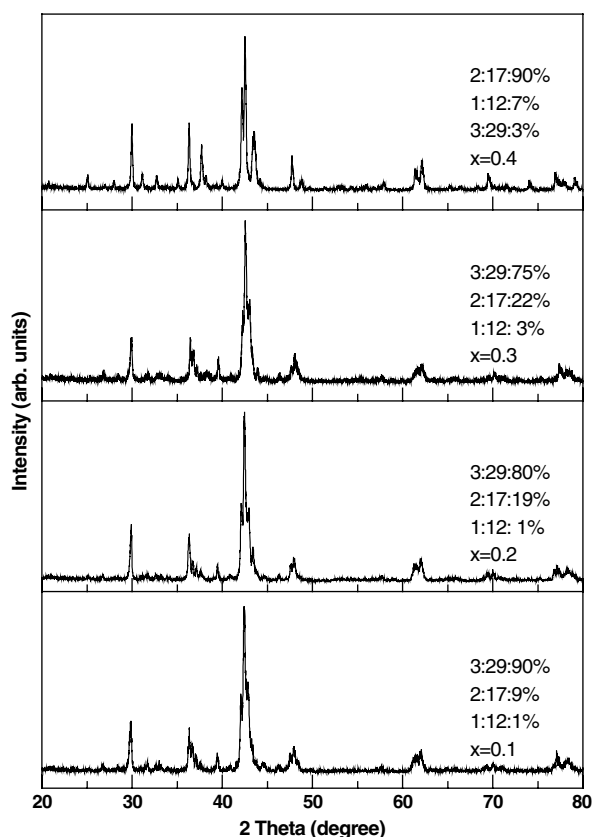
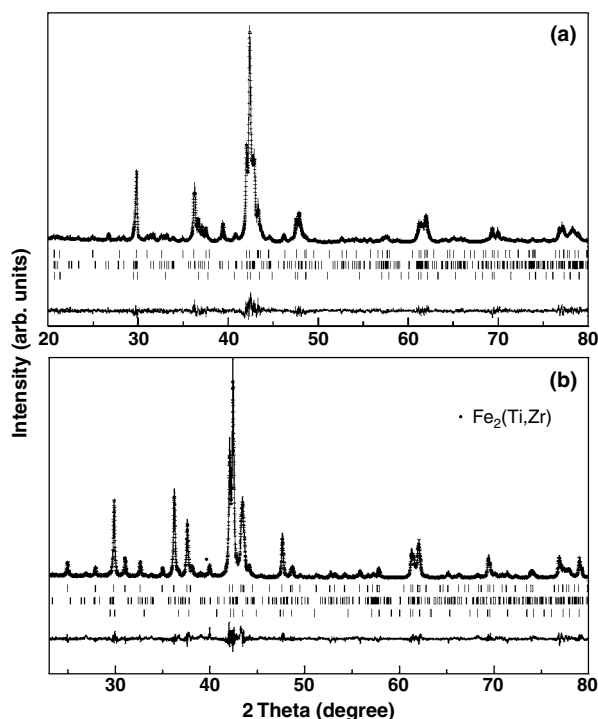


Figure 1. Comparison of XRD patterns of samples with different  $x$  (Zr content) values.

structure with the  $A2/m$  space group and a small amount of 2:17 phase and traces of 1:12 phase behave as impurities. Higher starting Zr contents make it more difficult to get the 3:29-type phase. When the starting Zr content  $x$  is  $\geq 0.4$ , the major phase is found to be rhombohedral  $\text{Th}_2\text{Zn}_{17}$ -type structure. For  $x \leq 0.3$ , the patterns can be quite well indexed in the monoclinic system with space group  $A2/m$ , while for  $x \geq 0.4$  the patterns can be quite well indexed in the rhombohedral system with space group  $R\bar{3}/m$ . As examples, the refinements of the XRD patterns for  $x = 0.2$  and  $0.5$  and the neutron patterns for  $x = 0.2$  and  $0.6$  are illustrated in figures 2 and 3, respectively. The lattice parameters and unit cell volumes of the 3:29 phase derived from the XRD patterns are shown in figure 4. It is revealed that the lattice parameters and the unit cell volumes decrease monotonically as the Zr contents increase. This clearly proves that most Zr atoms enter the R sublattice, since the atomic radius of Zr is smaller than that of R but larger than those of Fe and Ti. In contrast, if most Zr atoms substitute for Fe or Ti, the lattice parameters and the unit cell volumes will increase.

In order to find out whether Zr atoms enter the Nd sublattice or Fe sublattice, further investigation of the Zr occupancy is carried out by means of x-ray diffraction and neutron diffraction. It is accepted that stabilizing elements such as Ti and Mo prefer to occupy the three dumb-bell sites  $4i_1$ ,  $4i_2$  and  $4g$  among the eleven nonequivalent crystallographic sites in the Fe sublattice of  $\text{Nd}_3(\text{Fe}, \text{Ti})_{29}$ -type compound [10, 33]. These preferential occupancies may be determined by the site size effect (the volume of the site) and the thermodynamic



**Figure 2.** Results of the Rietveld analysis of the XRD patterns of compounds ((a):  $x = 0.2$ ;  $R_p = 8.10\%$ ,  $R_{wp} = 10.9\%$  and  $R_{exp} = 5.09\%$ ) and compounds ((b):  $x = 0.5$ ;  $R_p = 9.2\%$ ,  $R_{wp} = 11.9\%$ ,  $R_{exp} = 4.96\%$ ). The + signs represent the raw data. The solid line represents the calculated profile. Vertical bars indicate the positions of Bragg peaks for the 2:17, 3:29 and 1:12 phases, respectively. The lowest curve is the difference between the observed and calculated patterns.

effect (the atomic environment). The Fe atoms in the above-mentioned three sites have the largest average lengths of bonds with their nearest neighbouring Fe/M atoms. M atoms (such as Ti or Mo) generally have larger radius than Fe and they should enter those sites with the largest average bond lengths according to the site size effect. Moreover, M atoms have different affinities to rare earths and Fe. An estimate of these affinities can be obtained from the enthalpy of a mixture of two transition metals. The enthalpy of mixing for R–M is generally positive; however, that of Fe–M is usually negative. This means that Fe and M are more attractive, so the thermodynamic effect demands that M should occupy the sites with the smallest amounts of neighbouring rare earth atoms and the largest amounts of neighbouring Fe atoms [34]. The  $4i_1$ ,  $4i_2$  and  $4g$  sites meet this demand as well. Zr is similar to Ti and Mo since it has a larger radius than Fe and the enthalpy of mixing for Fe–Zr is negative ( $-118 \text{ kJ mol}^{-1}$  [35]). Therefore, if Zr enters an Fe sublattice, it should occupy the  $4i_1$ ,  $4i_2$  and  $4g$  sites like Ti or Mo. Because Ti and Fe make similar contributions to the XRD patterns, upon performing Rietveld refinement of the XRD patterns, only Zr atoms are put on the  $4i_1$ ,  $4i_2$  and  $4g$  sites and then the occupancies are refined as free parameters. The results show that there are no Zr atoms located at these dumb-bell sites.

Subsequently, the Rietveld refinements of XRD patterns are performed to study the Zr occupation in the Nd sublattice since the neutron scattering lengths of Nd and Zr are very close while the x-ray scattering contrast between them is relatively large. During the refinement, the

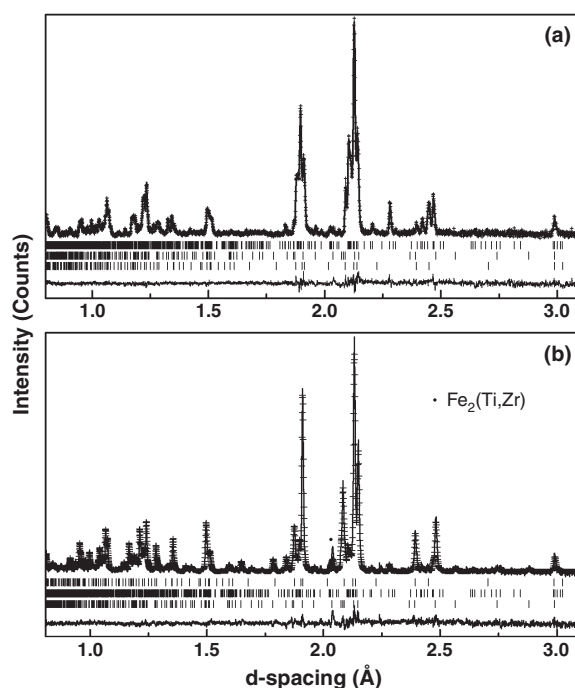


**Figure 3.** Time-of-flight neutron powder diffraction patterns (collected on SEPD of IPNS and refined by GSAS) of compounds ((a):  $x = 0.2$ ;  $wR_p = 3.59\%$ ,  $R_p = 2.82\%$ ) and compounds ((b):  $x = 0.6$ ;  $wR_p = 4.51\%$ ,  $R_p = 3.41\%$ ). The + signs represent the raw data. The solid line represents the calculated profile. Vertical bars indicate the positions of Bragg peaks for the 3:29, 2:17 and 1:12 phases. The background was fitted as a part of the refinement but has been subtracted prior to plotting. The lowest curve is the difference between the observed and calculated patterns.

Zr atoms are put on the R sites (2a and 4i) with the sum of the occupancies of Fe and Zr atoms on each of the two sites equalling 1 according to the nominal chemical concentration, and then the occupancies on these sites are set as free parameters; finally Ti atoms are put on the  $4i_1$ ,  $4i_2$  and 4g sites and the occupancies are fixed to the values obtained from the results from neutron diffraction patterns. The refinement results are listed in table 1. The final stoichiometries of the three 3:29-type compounds are  $\text{Nd}_{2.87}\text{Zr}_{0.13}\text{Fe}_{27.49}\text{Ti}_{1.52}$ ,  $\text{Nd}_{2.79}\text{Zr}_{0.21}\text{Fe}_{27.43}\text{Ti}_{1.53}$  and  $\text{Nd}_{2.67}\text{Zr}_{0.33}\text{Fe}_{27.55}\text{Ti}_{1.47}$ , respectively. The Zr contents obtained, 0.13, 0.21 and 0.33 per formula, are all larger than the nominal starting Zr contents. This suggests that Zr atoms actually enter the Nd sublattice exclusively, similarly to in the cases for the compounds of  $(\text{Nd}, \text{Zr})_2\text{Fe}_{17}$  [26],  $(\text{Nd}, \text{Zr})(\text{Fe}, \text{Mo})_{12}$  [28] and  $(\text{Gd}, \text{Zr})(\text{Fe}, \text{Mo})_{12}$  [29]. In conclusion, the Zr content partially substitutes for Nd and enters the 2a and 4i crystallographic sites in the structures of 3:29-type compounds; the maximum Zr content in the compound is about 0.33 per formula; higher Zr content will result in the transformation of the monoclinic  $\text{Nd}_3(\text{Fe}, \text{Ti})_{29}$ -type phase into a rhombohedral  $\text{Th}_2\text{Zn}_{17}$ -type one.

The measured Curie temperature  $T_C$  and saturation magnetization  $M_s$  at room temperature are presented in table 1. It shows that both the Curie temperatures and the saturation magnetizations decrease monotonically with increasing Zr content. It is known that both the crystal structure of a compound and the intrinsic magnetic properties of its constituent elements may affect the magnetic properties. In 3:29-type structure, the Fe(M)–Fe(M) bond length usually varies from 2.3 to 3.0 Å and the Fe–Fe interactions respond to the Fe–Fe bond length

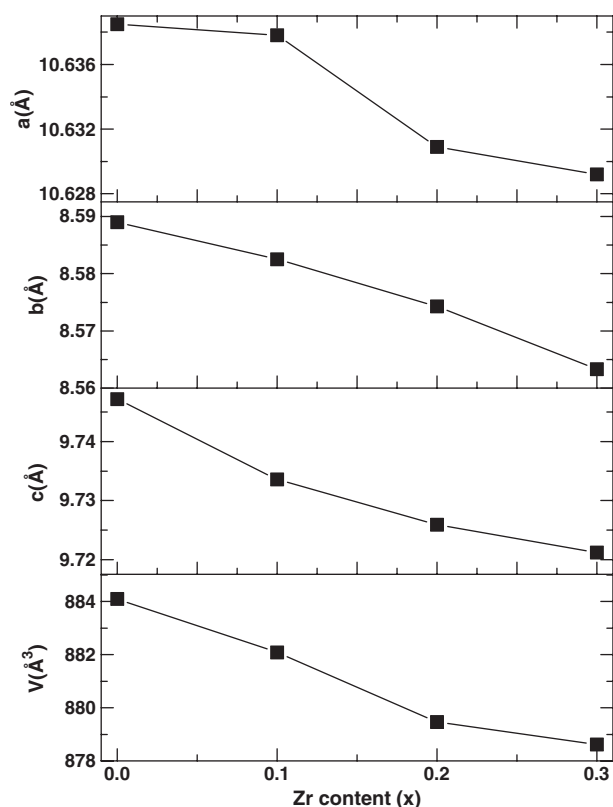


**Figure 4.** The dependence of the cell parameters of  $(\text{Nd}, \text{Zr})_3\text{Fe}_{27.5}\text{Ti}_{1.5}$  ( $0.1 \leq x \leq 0.3$ ) on the Zr content.

**Table 1.** The refinement results for XRD patterns and magnetic properties for the samples ( $x = 0.1, 0.2$  and  $0.3$ ).

$x$	Formula unit	Zr occupations	$T_C$ (K)	$M_s$ (RT) ( $\text{emu g}^{-1}$ )
0.1	$\text{Nd}_{2.87}\text{Zr}_{0.13}\text{Fe}_{27.48}\text{Ti}_{1.52}$	2a 0.014	435	118.3
		4i 0.019		
0.2	$\text{Nd}_{2.79}\text{Zr}_{0.21}\text{Fe}_{27.43}\text{Ti}_{1.57}$	2a 0.022	431	115.7
		4i 0.031		
0.3	$\text{Nd}_{2.67}\text{Zr}_{0.33}\text{Fe}_{27.53}\text{Ti}_{1.47}$	2a 0.032	423	113.6
		4i 0.051		

very sensitively. Fe moments with bond lengths less than  $2.45 \text{ \AA}$  are antiferromagnetically coupled and the Fe–Fe interactions are negative, whereas the Fe moments with bonds length larger than  $2.45 \text{ \AA}$  are ferromagnetically coupled and the Fe–Fe interactions are positive. The low Curie temperature  $T_C$  is usually due to the effect of negative exchange interactions between Fe atoms whose bond length is less than this critical value [36]. Rietveld analysis of the XRD patterns indicates contraction of the lattice parameters and the unit cell volumes when Zr is added to  $\text{Nd}_3(\text{Fe}, \text{Ti})_{29}$  compounds. This results in a decrease of the Fe–Fe bond lengths and it may lead to a decline of the Curie temperatures. Moreover, Zr bears no magnetic moment and

behaves only as a dilution element in intermetallic compounds; when more Zr is substituted for Nd, the Curie temperature as well as the saturation magnetization will decrease naturally.

#### 4. Conclusion

The maximum Zr content in  $\text{Nd}_3(\text{Fe}, \text{Ti})_{29}$  compound is about 0.33 per formula and higher Zr content will result in the transformation of the monoclinic  $\text{Nd}_3(\text{Fe}, \text{Ti})_{29}$ -type phase into the rhombohedral  $\text{Th}_2\text{Zn}_{17}$ -type one. Zr partially substitutes for Nd and enters the 2a and 4i sites at the Nd sublattice exclusively. With increasing Zr content, the lattice parameters  $a$ ,  $b$ ,  $c$  and the unit cell volumes  $V$  of  $(\text{Nd}, \text{Zr})_3(\text{Fe}, \text{Ti})_{29}$  compounds decrease monotonically and their intrinsic magnetic properties including Curie temperatures and saturation magnetizations lessen as well.

#### Acknowledgments

This work benefited from the use of SEPD at the Intense Pulsed Neutron Source at Argonne National Laboratory which is funded by the US Department of Energy, BES-Materials Science, under contract W-31-109-ENG-38. Financial support from the Chinese Academy of Sciences (Bai Ren Ji Hua) is greatly appreciated.

#### References

- [1] Ibarra M R, Morellon L, Blasco J, Pareti L, Algarabel P A, Garcia J, Albertini F and Paoluzi A 1994 *J. Phys.: Condens. Matter* **6** L717
- [2] Yang F, Nasunjilegal B, Wang J, Pan H, Qing W, Hu B, Wang Y, Liu G, Li H and Cadogan J M 1994 *J. Appl. Phys.* **76** 1971
- [3] Hu B P, Liu G C, Wang Y Z, Nasunjilegal B, Tang N, Yang F M, Li H S and Cadogan J M 1994 *J. Phys.: Condens. Matter* **6** L595
- [4] Fuerst C D, Pinkerton F E and Herbst J F 1994 *J. Appl. Phys.* **76** 6144
- [5] Han X F, Yang F M, Pan H G, Wang Y G, Wang J L, Liu H L, Zhao R W and Li H S 1997 *J. Appl. Phys.* **81** 7450
- [6] Ryan D H, Cadogan J M, Margarian A and Dunlop J B 1994 *J. Appl. Phys.* **76** 6150
- [7] Chu W G, Rao G H, Yang H F, Liu G Y and Liang J K 2001 *J. Phys.: Condens. Matter* **13** 441
- [8] Li H S, Cadogan J M, Davis R L, Margarian A and Dunlop J B 1994 *Solid State Commun.* **90** 487
- [9] Kalogirou O, Psycharis V, Saettas L and Niarchos D N 1995 *J. Magn. Magn. Mater.* **146** 335
- [10] Yelon W B and Hu Z 1996 *J. Appl. Phys.* **79** 1330
- [11] Hu Z, Yelon W B, Kalogirou O and Psycharis V 1996 *J. Appl. Phys.* **80** 2955
- [12] Gjoka M, Psycharis V, Kalogirou O, Sheloudko N, Niarchos D, Mikhov M, Dode J, Dilo T and Vyshka Sh 2000 *J. Alloys Compounds* **305** 311
- [13] Shah V R, Markandeyulu G, Rama Rao K V S, Huang M Q and McHenry M E 1999 *Solid State Commun.* **112** 161
- [14] Wang W Q, Wang J L, Liu B D, Li W X, Wu G H, Jin H M, Yang F M and De Boer F R 2002 *Physica B* **319** 52
- [15] Shah V R, Markandeyulu G, Rama Rao K V S, Huang M Q, Sirisha K and McHenry M E 2003 *Solid State Commun.* **352** 6
- [16] Wang W Q, Wang J L, Yan Y, Du X B, Wang W F and Jin H M 2003 *J. Appl. Comput.* **349** 23
- [17] Wang W Q, Wang J L, Fuquan B, Tang N, Wu G H, Yang F M and Jin H M 2001 *J. Phys. D: Appl. Phys.* **34** 3331
- [18] Wang W Q, Zhang X F, Su F, Wang X Q, Du X B, Jin H M, Yang F M and Wu G H 2003 *Chem. J. Chin. Univ.* **1** 13
- [19] Sheloudko N, Gjoka M, Kalogirou O, Niarchos D, Skumryev V, Hadjipanayis G, Surinach S and Munoz J S 2003 *J. Alloys Compounds* **352** 73
- [20] Huang F, Liang J K, Liu Q L, Chen X L and Chen Y 2000 *J. Phys. D: Appl. Phys.* **33** 780
- [21] Huang F, Liang J K, Liu Q L, Chen X L and Chen Y 1999 *J. Appl. Comput.* **291** 239



- [22] de Rango P, Rivoirard S, Traverse A, Fruchart D and Genin F N 2003 *J. Appl. Comput.* **356/357** 579
- [23] McGuinness P J, Skulj I, Porenta A and Kobe S 1998 *J. Magn. Magn. Mater.* **188** 199
- [24] Lefevrea A, Cohen-Adada M Th and Mentzen B F 1997 *J. Appl. Comput.* **256** 207
- [25] Chen Z C, Hadjipanayis G C, Daniel M, Digas M, Moukarika A and Papaefthymiou V 1998 *J. Magn. Magn. Mater.* **177-181** 1109
- [26] Al-Omari I A, Yeshurun Y, Jaswal S S, Zhou J and Sellmyer D J 2000 *J. Magn. Magn. Mater.* **217** 83
- [27] Hao S Q, Chen N X and Shen J 2002 *J. Appl. Comput.* **343** 53
- [28] Du H L, Han J Z, Zhang W Y, Wang C S, Wang W C, Liu S Q, Chen H Y, Zhang X D and Yang Y C 2004 *J. Magn. Magn. Mater.* **283** 316
- [29] Zinkevich M, Mattern N, Bacher I and Puerta S 2002 *J. Appl. Comput.* **336** 320
- [30] Derkaoui S, Valignat N and Allibert C H 1996 *J. Magn. Magn. Mater.* **232** 296
- [31] Rodriguez-Carjaval J 2001 *An Introduction to the Program FULLPROF2000 (Version July 2001)* ed J Rodriguez-Carjaval (France: Laboratoire Leon Brillouin (CEA-CNRS))
- [32] Larson A C and Von Dreele R B 2000 *General Structure Analysis System (GSAS)* ed A C Larson and R B Von Dreele, Los Alamos National Laboratory LAUR
- [33] Pan H G 2002 *Formation, Structure and Intrinsic Magnetic Properties of the  $R_3(Fe, Mo)_{29}$  Intermetallic Compounds* (Beijing, China: Higher Education Press) p 93
- [34] Liang J K, Liu Q L, Huang F, Rao G H and Chen X L 2001 *Prog. Nat. Sci.* **11** 1132
- [35] Ping D H, Wu Y Q, Hono K, Willard M A, McHenry M E and Laughlin D E 2001 *Scr. Mater.* **45** 781
- [36] Gvord D and Lemaire R 1974 *IEEE. Trans. Magn.* **10** 109